

A Fast Iterative Method for Removing Sparse Noise from Sparse Signals

Sahar Sadrizadeh, Ehsan Asadi, and Farokh Marvasti

Abstract—In this paper, we propose a new method to reconstruct a signal corrupted by noise where both signal and noise are sparse but in different domains. The problem investigated in this paper arises in different applications such as impulsive noise cancellation from images and audios, and decomposition of low-rank and sparse components of matrices. First, we provide a cost function for our problem and then present an iterative method to find its local minimum. The convergence analysis of the algorithm is also provided. As an application of this problem, we apply our algorithm for impulsive noise (salt-and-pepper noise and random-valued impulsive noise) removal from images and compare our results with other notable algorithms in the literature. Furthermore, we apply our algorithm for removing clicks from audio signals. Simulation results show that our algorithms is simple and fast, and it outperforms the other state-of-the-art methods in terms of reconstruction quality and/or complexity.

Index Terms—Adaptive thresholding, image denoising, iterative method, impulsive noise, sparse signal.

I. INTRODUCTION

THE problem considered in this paper can be modeled as:

$$\mathbf{Y} = \mathcal{D}^{-1}(\tilde{\mathbf{X}}) + \tilde{\mathbf{N}}, \quad (1)$$

where the original sparse signal $\tilde{\mathbf{X}} \in \mathbb{R}^{m \times n}$ is corrupted additively by sparse noise $\tilde{\mathbf{N}} \in \mathbb{R}^{m \times n}$, and \mathcal{D} is the domain in which the signal is sparse; in other words, the signal and the noise are both sparse but in different domains. We aim to reconstruct the original signal by cancelling the impulsive noise from the observed signal \mathbf{Y} .

Salt-and-pepper noise and random-valued impulsive noise (two of the most common types of sparse noise) are common phenomenon in image processing, audio and video transition [1]–[6], laser sensors [7], and data transition over noisy communication channels [8], [9] such as underwater acoustic channels and power line channels. Additionally, in the random missing sample problem [10] when no side information about the location of missing samples is available, the random missing samples can be considered as sparse noise, and thus the problem can be modeled by problem (1). The problem stated in (1) also arises in low-rank and sparse matrix decomposition since the singular values of a low-rank matrices are sparse. [11]–[13].

Various methods have been proposed for impulsive noise cancellation from 1-D and 2-D signals. Most of these methods are intended for low-pass signals and image denoising. All

the algorithms related to the impulsive noise removal can be divided into two general categories:

1) Methods which first detect the corrupted samples, and then restore them from other clean samples. In the case of salt-and-pepper noise, most of the research are from the this category and usually result in a better reconstruction since they first find the mask matrix with which the signal is corrupted [2], [14]–[20]. These methods have two drawbacks. When the original signal is corrupted with random-valued impulsive noise, the detection of noisy pixels becomes very challenging. In addition, all these methods utilize the structure of the image (mainly its low-pass characteristic) to detect the location of corrupted pixels and hence they are not applicable to signals other than images. As examples of the first category, a modified version of median filter, Modified Decision Based Unsymmetric Trimmed Median Filter (MDBUTMF), which is only applied to the noisy pixels of the image is presented in [14]. Inpainting of audio signals corrupted by impulsive noise is considered in [15]. It is assumed that the location of the distorted data is known and the audio signal is reconstructed through sparse recovery techniques. In [2], noisy pixels are detected through an impulse detector and the image is restored by applying a weighted-average filter. The authors of [16] present a two-step algorithm. In the first step the noisy pixels are detected by Support Vector Machine (SVM) classification, and then they are restored by applying an adaptive fuzzy filter.

2) Methods which detect and restore the noisy pixels simultaneously [1], [19], [21]–[27]. The method presented in this paper falls into this category and we compare our results with other algorithms of this class. Examples of this category are as follows: In [21], the Adaptive Median Filter (AMF) is introduced for impulsive noise removal from images. In this algorithm, the window size of the median filter is adjusted according to the impulsive noise density. An Adaptive Median Filter which utilizes the Center-Weighted median (ACWMF) is introduced in [28], and unlike other median-based filters, it performs well in the presence of random valued impulsive noise. In [29], the Weighted Encoding With Sparse Nonlocal Regularization method (WESNR) is introduced which integrates a soft impulse detection and sparse non-local prior to remove mixed noise from images. The authors of [24] present a method based on Bayesian inference for impulsive noise removal from audio signals. For restoring images corrupted by impulsive noise, a method is suggested in [25] which utilizes particle swarm optimization and fuzzy filtering. The Structure-Adaptive Fuzzy Estimation (SAFE) algorithm is introduced in [27], in which the random-valued impulsive noise is removed via Gaussian Maximum Likelihood Estimation. The structure information of the image is incorporated into this algorithm

S. Sadrizadeh, E.Asadi, and F. Marvasti are with the Advanced Communication Research Institute (ACRI), Electrical Engineering Department, Sharif University of Technology, Tehran, Iran (email: ss.sadrizadeh@ee.sharif.edu; ehsan.asadikangarshahi@epfl.ch; marvasti@sharif.edu).

as the fuzziness metrics in the form of point reliability and structure similarity. The annihilating filter-based low-rank Hankel matrix approach (ALPHA) is proposed in [30]. This method models the impulsive noise as a sparse component, and the underlying image as a low-rank Hankel structured matrix.

In this paper, a new iterative method is proposed which is applicable to 1-D and 2-D sparse signals; moreover, it reconstructs both the signal corrupted by sparse noise such as salt-and-pepper and random-valued impulsive noise, by contrast to most of the other methods which are applicable to one of these noises, without detecting the noisy samples beforehand. Our method reconstructs both signal and noise iteratively by thresholding them in their corresponding sparse domains and projecting them onto the set imposed by (1).

The rest of this paper is organized as follows. In Section II, first, an optimization problem is suggested then our method which tries to minimise this cost function is introduced and analyzed, and some modifications are presented for the image denoising context. Section III summarizes the simulation results. We also compare our results with other methods in the impulsive noise cancellation literature. Finally, the paper is concluded in Section IV.

II. THE PROPOSED METHOD

A. Problem Formulation

First, we start with defining some useful variables. W is defined as the set of all pairs (\mathbf{X}, \mathbf{N}) satisfying (1):

$$W \triangleq \{(\mathbf{X}, \mathbf{N}) | \mathbf{X}, \mathbf{N} \in \mathbb{R}^{m \times n}, \mathbf{Y} = \mathcal{D}^{-1}(\mathbf{X}) + \mathbf{N}\}; \quad (2)$$

$(\tilde{\mathbf{X}}, \tilde{\mathbf{N}})$ with respective sparsity numbers $(\tilde{k}_1, \tilde{k}_2)$ is the unique sparsest member of W if there is no other member of W with sparsity numbers (k_1, k_2) where $k_1 + k_2 \leq \tilde{k}_1 + \tilde{k}_2$. Therefore we have:

$$\begin{aligned} (\tilde{\mathbf{X}}, \tilde{\mathbf{N}}) \text{ is the unique sparsest member of } W &\Leftrightarrow \\ \forall (\mathbf{X}, \mathbf{N}) \in W, (\mathbf{X}, \mathbf{N}) \neq (\tilde{\mathbf{X}}, \tilde{\mathbf{N}}) : k_1 + k_2 > \tilde{k}_1 + \tilde{k}_2. & \quad (3) \end{aligned}$$

Furthermore, the function $f_\lambda(\mathbf{X}, \mathbf{N}, \mathbf{T}_1, \mathbf{T}_2)$ is defined as:

$$\begin{aligned} f_\lambda(\mathbf{X}, \mathbf{N}, \mathbf{T}_1, \mathbf{T}_2) &\triangleq \|(\mathbf{1} - \mathbf{T}_1) \odot \mathbf{X}\|_F^2 + \|(\mathbf{1} - \mathbf{T}_2) \odot \mathbf{N}\|_F^2 \\ &\quad + \lambda(\|\text{vec}(\mathbf{T}_1)\|_1 + \|\text{vec}(\mathbf{T}_2)\|_1), \end{aligned} \quad (4)$$

where $(\mathbf{X}, \mathbf{N}) \in W$, $\mathbf{T}_1, \mathbf{T}_2$ are $m \times n$ binary matrices, and $\mathbf{1}$ is a matrix of ones. \odot represents the Hadamard (entry-wise) product of matrices and $\|\text{vec}(\cdot)\|_1$ denotes the entry-wise ℓ_1 norm (or the ℓ_1 norm of the vectorization) of the input matrix.

Our objective can be summarized as the following optimization problem:

$$\begin{aligned} \underset{(\mathbf{X}, \mathbf{N}), (\mathbf{T}_1, \mathbf{T}_2)}{\text{argmin}} \quad & f_\lambda(\mathbf{X}, \mathbf{N}, \mathbf{T}_1, \mathbf{T}_2). \\ \text{s.t.} \quad & (\mathbf{X}, \mathbf{N}) \in W. \end{aligned} \quad (5)$$

This claim will be proved in Theorem 1, but as an intuition, we aim to find the sparsest member of the set W , i.e., the member with minimum $\lambda(\|\text{vec}(\mathbf{T}_1)\|_1 + \|\text{vec}(\mathbf{T}_2)\|_1)$, where the components outside the supports $(\mathbf{T}_1, \mathbf{T}_2)$ shrink, i.e., $\|(\mathbf{1} - \mathbf{T}_1) \odot \mathbf{X}\|_F^2 + \|(\mathbf{1} - \mathbf{T}_2) \odot \mathbf{N}\|_F^2$ is minimized. It is worth mentioning that this function is convex *w.r.t* (\mathbf{X}, \mathbf{N}) since the

feasible region is a convex set, and the objective function is a quadratic function of (\mathbf{X}, \mathbf{N}) when $(\mathbf{T}_1, \mathbf{T}_2)$ are fixed.

Finally, we will define ε as follows: For a specific pair of binary matrices $(\mathbf{T}_1, \mathbf{T}_2)$, the matrices minimizing f_λ are denoted by $(\mathbf{X}^*, \mathbf{N}^*)$. There exists only finite numbers $(2^{m \times n} \times 2^{m \times n})$ of 4-tuples $(\mathbf{X}^{*i}, \mathbf{N}^{*i}, \mathbf{T}_1^i, \mathbf{T}_2^i)$, which are distinguished by superscript i . As previously mentioned, the solution of the optimization problem (5) is one of these 4-tuples which minimizes the cost function. The minimum non-zero value of $\|(\mathbf{1} - \mathbf{T}_1) \odot \mathbf{X}^*\|_F^2 + \|(\mathbf{1} - \mathbf{T}_2) \odot \mathbf{N}^*\|_F^2$ among these 4-tuples is denoted by ε . Mathematically, ε is defined as:

$$\begin{aligned} \varepsilon &\triangleq \min_i \|(\mathbf{1} - \mathbf{T}_1^i) \odot \mathbf{X}^{*i}\|_F^2 + \|(\mathbf{1} - \mathbf{T}_2^i) \odot \mathbf{N}^{*i}\|_F^2. \\ \text{s.t.} \quad & \|(\mathbf{1} - \mathbf{T}_1^i) \odot \mathbf{X}^{*i}\|_F^2 + \|(\mathbf{1} - \mathbf{T}_2^i) \odot \mathbf{N}^{*i}\|_F^2 \neq 0. \end{aligned} \quad (6)$$

Theorem 1. *Let ε be defined as (6). Also let the unique sparsest element of W defined by (3) be $(\tilde{\mathbf{X}}, \tilde{\mathbf{N}})$ with respective supports $(\tilde{\mathbf{T}}_1, \tilde{\mathbf{T}}_2)$; moreover let the sparsity numbers of $(\tilde{\mathbf{X}}, \tilde{\mathbf{N}})$ be $(\tilde{k}_1, \tilde{k}_2)$, then for $\lambda < \varepsilon/(\tilde{k}_1 + \tilde{k}_2)$, the minimizer of $f_\lambda(\mathbf{X}, \mathbf{N}, \mathbf{T}_1, \mathbf{T}_2)$ over W is $(\tilde{\mathbf{X}}, \tilde{\mathbf{N}}, \tilde{\mathbf{T}}_1, \tilde{\mathbf{T}}_2)$.*

Proof: Before we proceed with the proof, let $(\mathbf{X}^*, \mathbf{N}^*)$ with respective sparsity numbers of (k_1, k_2) be the minimizers of f_λ for a given pair of $(\mathbf{T}_1, \mathbf{T}_2)$. We will show that the cost function (4) has greater values for binary matrices $(\mathbf{T}_1, \mathbf{T}_2)$ other than $(\tilde{\mathbf{T}}_1, \tilde{\mathbf{T}}_2)$. To this aim, we consider two cases:

Case 1:

$$\|(\mathbf{1} - \mathbf{T}_1) \odot \mathbf{X}^*\|_F = 0 \wedge \|(\mathbf{1} - \mathbf{T}_2) \odot \mathbf{N}^*\|_F = 0 \quad (7)$$

Case 2:

$$\|(\mathbf{1} - \mathbf{T}_1) \odot \mathbf{X}^*\|_F \neq 0 \vee \|(\mathbf{1} - \mathbf{T}_2) \odot \mathbf{N}^*\|_F \neq 0 \quad (8)$$

In the first case, we will show that $\|\text{vec}(\mathbf{T}_1)\|_1 + \|\text{vec}(\mathbf{T}_2)\|_1 \geq \tilde{k}_1 + \tilde{k}_2$. Assume the opposite, that is:

$$\|\text{vec}(\mathbf{T}_1)\|_1 + \|\text{vec}(\mathbf{T}_2)\|_1 \leq \tilde{k}_1 + \tilde{k}_2 - 1, \quad (9)$$

then $(\mathbf{1} - \mathbf{T}_1)$ and $(\mathbf{1} - \mathbf{T}_2)$ has at most $\tilde{k}_1 + \tilde{k}_2 - 1$ zero entries in total. Therefore, in order for (7) to be true, \mathbf{X}^* and \mathbf{N}^* can have at most $\tilde{k}_1 + \tilde{k}_2 - 1$ non-zero entries in the corresponding zero elements of $(\mathbf{1} - \mathbf{T}_1)$ and $(\mathbf{1} - \mathbf{T}_2)$ respectively, in other words:

$$\begin{aligned} \|\text{vec}(\mathbf{X}^*)\|_0 + \|\text{vec}(\mathbf{N}^*)\|_0 &\leq \tilde{k}_1 + \tilde{k}_2 - 1 \Rightarrow \\ k_1 + k_2 &\leq \tilde{k}_1 + \tilde{k}_2 - 1. \end{aligned} \quad (10)$$

Based on the assumption of the uniqueness of the sparsest solution, the sum of the sparsity numbers of every members of W , except the sparsest one, is more than $\tilde{k}_1 + \tilde{k}_2$; then since $(\mathbf{X}^*, \mathbf{N}^*) \in W$, a contradiction is found. Consequently $\|\text{vec}(\mathbf{T}_1)\|_1 + \|\text{vec}(\mathbf{T}_2)\|_1 \geq \tilde{k}_1 + \tilde{k}_2$, and the equality only holds for the sparsest member.

In the second case, since (8) holds according to the definition ε in (6):

$$\|(\mathbf{1} - \mathbf{T}_1^i) \odot \mathbf{X}^{*i}\|_F^2 + \|(\mathbf{1} - \mathbf{T}_2^i) \odot \mathbf{N}^{*i}\|_F^2 \geq \varepsilon > \lambda(\tilde{k}_1 + \tilde{k}_2). \quad (11)$$

One can easily see that in both cases, for all the members of W , except for the sparsest one, $f_\lambda(\mathbf{X}, \mathbf{N}, \mathbf{T}_1, \mathbf{T}_2) > \lambda(\tilde{k}_1 +$

$\tilde{k}_2) = f_\lambda(\tilde{\mathbf{X}}, \tilde{\mathbf{N}}, \tilde{\mathbf{T}}_1, \tilde{\mathbf{T}}_2)$. Hence the minimizer of f_λ is indeed the sparsest member of W . ■

Now we discuss the uniqueness of the sparsest member of W in Theorem 2.

Theorem 2. *The sparsest member of W with sparsity numbers $(\tilde{k}_1, \tilde{k}_2)$ is unique, if the following sufficient conditions are satisfied:*

$$\begin{cases} \mathbf{B}^T \otimes \mathbf{A} \text{ is orthonormal} \\ \tilde{k}_1 + \tilde{k}_2 < \frac{1}{2}(1 + M^{-1}) \end{cases}; \quad (12)$$

where $(\cdot)^T$ and \otimes denote the transpose of a matrix and the Kronecker product of two matrices respectively; the linear transformation $\mathcal{D}^{-1}(\mathbf{X}) = \mathbf{A}\mathbf{X}\mathbf{B}$; M is the mutual coherence of two orthonormal bases \mathbf{I} and $\mathbf{B}^T \otimes \mathbf{A}$, which is defined as the maximum absolute value of the inner-products between the columns of these two matrices and since one the bases is Identity the M equals the maximum absolute value of the elements of $\mathbf{B}^T \otimes \mathbf{A}$.

Proof: Assume otherwise, that is, assume that there exists two members in W with sparsity numbers $(\tilde{k}_1, \tilde{k}_2)$ and they are denoted by $(\mathbf{X}_1, \mathbf{N}_1)$ and $(\mathbf{X}_2, \mathbf{N}_2)$.

$$\begin{aligned} \mathcal{D}^{-1}(\mathbf{X}_1) + \mathbf{N}_1 &= \mathcal{D}^{-1}(\mathbf{X}_2) + \mathbf{N}_2 = \mathbf{Y} \Rightarrow \\ \mathcal{D}^{-1}(\mathbf{X}_1 - \mathbf{X}_2) + (\mathbf{N}_1 - \mathbf{N}_2) &= \mathbf{0} \Rightarrow \\ \mathbf{A}(\mathbf{X}_1 - \mathbf{X}_2)\mathbf{B} + (\mathbf{N}_1 - \mathbf{N}_2) &= \mathbf{0}; \end{aligned} \quad (13)$$

by defining $\mathbf{X}' = \mathbf{X}_1 - \mathbf{X}_2$ and $\mathbf{N}' = \mathbf{N}_1 - \mathbf{N}_2$, with maximum sparsity numbers of $2\tilde{k}_1$ and $2\tilde{k}_2$ respectively, we will have:

$$\begin{aligned} \mathbf{A}\mathbf{X}'\mathbf{B} + \mathbf{N}' &= \mathbf{0} \Rightarrow \\ \text{vec}(\mathbf{A}\mathbf{X}'\mathbf{B}) + \text{vec}(\mathbf{N}') &= \mathbf{0} \Rightarrow \\ (\mathbf{B}^T \otimes \mathbf{A})\text{vec}(\mathbf{X}') + \text{vec}(\mathbf{N}') &= \mathbf{0}; \end{aligned} \quad (14)$$

if $\mathbf{x} = \text{vec}(\mathbf{X}')$, $\mathbf{n} = \text{vec}(\mathbf{N}')$ and $\mathbf{C} = \mathbf{B}^T \otimes \mathbf{A} \in \mathbb{R}^{mn \times mn}$ we have to investigate the following equation:

$$\begin{cases} \mathbf{C}\mathbf{x} + \mathbf{n} = \mathbf{0} \\ \mathbf{x}, \mathbf{n} \in \mathbb{R}^{mn \times 1} \end{cases}. \quad (15)$$

We can conclude that:

$$\mathbf{x} = -\mathbf{C}^{-1}\mathbf{n} = -\mathbf{C}^T\mathbf{n}; \quad (16)$$

in other words, $-\mathbf{n}$ is the representation of \mathbf{x} in the orthonormal basis \mathbf{C} . According to Theorem 7.3 in [31], if \mathbf{x} have N_I and N_C non-zero coefficients in orthonormal bases \mathbf{I} and \mathbf{C} respectively, then $N_I + N_C \geq (1 + M^{-1})$. Therefore:

$$\begin{aligned} \|\mathbf{x}\|_0 + \|\mathbf{n}\|_0 &\Rightarrow \\ 2\tilde{k}_1 + 2\tilde{k}_2 &\geq (1 + M^{-1}); \end{aligned} \quad (17)$$

which contradicts (12). Hence $\mathbf{x} = \mathbf{0}$ and $\mathbf{n} = \mathbf{0}$. Since \mathbf{x} and \mathbf{n} are the vectorization of \mathbf{X}' and \mathbf{N}' respectively, $\mathbf{X}' = \mathbf{X}_1 - \mathbf{X}_2 = \mathbf{0}$ and $\mathbf{N}' = \mathbf{N}_1 - \mathbf{N}_2 = \mathbf{0}$. The uniqueness of the sparsest member of W is then concluded. ■

Algorithm 1 IDT

```

1: Input:
2:   Observed matrix:  $\mathbf{Y} \in \mathbb{R}^{m \times n}$ 
3:   Maximum number of iterations of the outer loop:  $K$ 
4:   Decreasing sequence:  $\mathbf{th} \in \mathbb{R}^K$ 
5:   Stopping threshold of the inner loop:  $\delta$ 
6: Output:
7:   Recovered estimate of the signal:  $\hat{\mathbf{X}} \in \mathbb{R}^{m \times n}$ 
8:   Recovered estimate of the noise:  $\hat{\mathbf{N}} \in \mathbb{R}^{m \times n}$ 
9: procedure
10:   $\hat{\mathbf{X}} \leftarrow \mathcal{D}(\mathbf{Y}), \quad \hat{\mathbf{N}} \leftarrow \mathbf{0}$ 
11:  for  $k = 1 : K$  do
12:     $\mathbf{X}^0 \leftarrow \hat{\mathbf{X}}, \quad \mathbf{N}^0 \leftarrow \hat{\mathbf{N}}, \quad l \leftarrow 0$ 
13:     $\sqrt{\lambda} \leftarrow \mathbf{th}_k$ 
14:    while  $e > \delta$  do
15:       $\mathbf{X}^l \leftarrow \text{threshold}(|\mathbf{X}_{i,j}^l|_{i=1,j=1}^{m,n}, \sqrt{\lambda})$ 
16:       $\mathbf{N}^l \leftarrow \text{threshold}(|\mathbf{N}_{i,j}^l|_{i=1,j=1}^{m,n}, \sqrt{\lambda})$ 
17:       $\mathbf{X}^{l+1} \leftarrow 0.5 (\mathbf{X}^l + \mathcal{D}(\mathbf{Y} - \mathbf{N}^l))$ 
18:       $\mathbf{N}^{l+1} \leftarrow 0.5 (-\mathcal{D}^{-1}(\mathbf{X}^l) + \mathbf{Y} + \mathbf{N}^l)$ 
19:       $e \leftarrow \|\mathbf{N}^{l+1} - \mathbf{N}^l\|_F$ 
20:       $l \leftarrow l + 1$ 
21:    end while
22:     $\hat{\mathbf{X}} \leftarrow \mathbf{X}^l$ 
23:     $\hat{\mathbf{N}} \leftarrow \mathbf{N}^l$ 
24:  end for
25:  return  $\hat{\mathbf{X}}, \hat{\mathbf{N}}$ 
26: end procedure

```

B. Algorithm

Now, we present our algorithm and discuss how the minimum of f_λ can be found iteratively. The procedure of our algorithm is given in Algorithm 1 with the name Iterative Double Thresholding (IDT).

For a fixed value of λ (in the inner loop of the algorithm), let \mathbf{X}^l and \mathbf{N}^l denote the recovered signal and noise after l iterations. One can easily calculate the minimizer of f_λ w.r.t binary matrices $(\hat{\mathbf{T}}_1, \hat{\mathbf{T}}_2)$ by thresholding $(\mathbf{X}^l, \mathbf{N}^l)$ as follows:

$$\begin{aligned} (\hat{\mathbf{T}}_1)_{i,j} &= \begin{cases} 0, & (\mathbf{X}^l)_{i,j} < \sqrt{\lambda} \\ 1, & (\mathbf{X}^l)_{i,j} \geq \sqrt{\lambda} \end{cases}, \\ (\hat{\mathbf{T}}_2)_{i,j} &= \begin{cases} 0, & (\mathbf{N}^l)_{i,j} < \sqrt{\lambda} \\ 1, & (\mathbf{N}^l)_{i,j} \geq \sqrt{\lambda} \end{cases}, \end{aligned} \quad (18)$$

where $(\cdot)_{i,j}$ is the element of matrix at the intersection of i -th row and j -th column.

A new pair of \mathbf{X}^l and \mathbf{N}^l (which is not necessarily in W) is attained by considering $(\hat{\mathbf{T}}_1, \hat{\mathbf{T}}_2)$ to be their respective supports as follows:

$$\mathbf{X}^l = \hat{\mathbf{T}}_1 \odot \mathbf{X}^l, \quad \mathbf{N}^l = \hat{\mathbf{T}}_2 \odot \mathbf{N}^l. \quad (19)$$

Inserting (18) in (19) is equivalent to thresholding the entries of \mathbf{X}^l and \mathbf{N}^l by $\sqrt{\lambda}$. This is done in the lines 15 and 16 of Algorithm 1, where $\text{threshold}(|\mathbf{A}_{i,j}|_{i=1,j=1}^{m,n}, th)$ represents thresholding the entries of matrix \mathbf{A} based on their absolute values with regard to the threshold level of th .

Now we have to project this pair onto the set W so that the condition of the problem (5) is met. It is obvious from Pythagorean theorem that projecting decreases the value of f_λ . In order to compute this projection, we denote the concatenation of two matrices \mathbf{U}, \mathbf{V} by $[\mathbf{U}, \mathbf{V}]$, and show the Frobenius inner product of two matrices, i.e., trace of their product, by $\langle \mathbf{U}, \mathbf{V} \rangle$.

Lemma 1. *If \mathcal{D} is an orthogonal transformation, then $\langle [\mathcal{D}(\mathbf{U}), \mathbf{U}], [\mathcal{D}(-\mathbf{V}), \mathbf{V}] \rangle = 0$.*

Proof:

$$\begin{aligned} \langle [\mathcal{D}(\mathbf{U}), \mathbf{U}], [\mathcal{D}(-\mathbf{V}), \mathbf{V}] \rangle &= \langle \mathcal{D}(\mathbf{U}), \mathcal{D}(-\mathbf{V}) \rangle + \langle \mathbf{U}, \mathbf{V} \rangle \\ &= \langle \mathbf{U}, -\mathbf{V} \rangle + \langle \mathbf{U}, \mathbf{V} \rangle = 0. \end{aligned} \quad (20)$$

The second equality in (20) holds because of the orthogonality of the \mathcal{D} transformation. ■

In order for $(\hat{\mathbf{X}}, \hat{\mathbf{N}})$ to be the projection of (\mathbf{X}, \mathbf{N}) onto the set W , the error $(\mathbf{X}, \mathbf{N}) - (\hat{\mathbf{X}}, \hat{\mathbf{N}})$ has to be orthogonal to the set, i.e., it has to be orthogonal to the difference of any two members of W . The difference of any two members of W is $(\mathcal{D}(\mathbf{Y} - \mathbf{U}_1), \mathbf{U}_1) - (\mathcal{D}(\mathbf{Y} - \mathbf{U}_2), \mathbf{U}_2) = (\mathcal{D}(\mathbf{U}_2 - \mathbf{U}_1), \mathbf{U}_1 - \mathbf{U}_2)$, which is of the form $(\mathcal{D}(-\mathbf{V}), \mathbf{V})$. By employing Lemma 1, the error $(\mathbf{X}, \mathbf{N}) - (\hat{\mathbf{X}}, \hat{\mathbf{N}})$ has to be of the form $(\mathcal{D}(\mathbf{U}), \mathbf{U})$ so that the orthogonality is assured. Specifically:

$$\begin{cases} (\mathbf{X}, \mathbf{N}) - (\hat{\mathbf{X}}, \hat{\mathbf{N}}) = (\mathcal{D}(\mathbf{U}), \mathbf{U}) \\ \mathcal{D}^{-1}(\hat{\mathbf{X}}) + \hat{\mathbf{N}} = \mathbf{Y} \end{cases} \quad (21)$$

The first equality holds as a result of Lemma 1. The second equality also holds since $(\hat{\mathbf{X}}, \hat{\mathbf{N}}) \in W$. One can easily omit the auxiliary variable \mathbf{U} and obtain the following results:

$$\begin{cases} \hat{\mathbf{X}} = 0.5 (\mathbf{X} + \mathcal{D}(\mathbf{Y} - \mathbf{N})) \\ \hat{\mathbf{N}} = 0.5 (-\mathcal{D}^{-1}(\mathbf{X}) + \mathbf{Y} + \mathbf{N}) \end{cases} \quad (22)$$

The process of projection (22) is carried out in lines 17 and 18 of Algorithm 1.

Theorem 1 only holds for small enough λ and in this case, the optimization problem (5) is highly non-convex. Therefore, the use of warm start is necessary, i.e. we start with large values of λ and iteratively find the local minimum of f_λ in the inner loop of the algorithm, then this estimation will be used as an initial guess for the next optimization problem with smaller λ . This procedure is continued until λ meet the conditions of Theorem 1, and hence the sparsest solution of problem 1, which is the minimizer of f_λ , is achieved.

C. Modifications

In this subsection, we proceed to introduce some modifications to our algorithm. The modified algorithm can be found in Algorithm 2. Note that the lines of the algorithm marked with (*) are only for image denoising and should be omitted in other applications. It is seen through simulation results that these modifications improve the reconstruction quality.

In this algorithm, the inner loop and outer loop are merged. Furthermore, in the first algorithm, the signal and noise are

Algorithm 2 Modified IDT

```

1: Input:
2:   Observed matrix:  $\mathbf{Y} \in \mathbb{R}^{m \times n}$ 
3:   Four constants:  $\alpha_1, \beta_1, \alpha_2, \beta_2$ 
4:   Standard deviation of the gaussian filter:  $\sigma$  (*)
5:   Maximum number of iterations:  $K$ 
6:   Stopping threshold:  $\delta$ 
7: Output:
8:   Recovered estimate of the signal:  $\hat{\mathbf{X}} \in \mathbb{R}^{m \times n}$ 
9:   Recovered estimate of the noise:  $\hat{\mathbf{N}} \in \mathbb{R}^{m \times n}$ 
10: procedure
11:    $\mathbf{X}^0 \leftarrow \mathcal{D}(\mathbf{Y}), \quad \mathbf{N}^0 \leftarrow 0, \quad k \leftarrow 0$ 
12:   while  $e > \delta$  &  $k \leq K$  do
13:      $\mathbf{X}^k \leftarrow \text{threshold}(|\mathbf{X}_{i,j}^k|_{i=1,j=1}^{m,n}, \beta_1 e^{-\alpha_1 k})$  (*)
14:      $\mathbf{X}^k \leftarrow \text{clip}(\mathcal{D}^{-1}(\mathbf{X}^k))$  (*)
15:      $\mathbf{X}^k \leftarrow \text{gaussian-filter}(\mathbf{X}^k, \sigma)$  (*)
16:      $\mathbf{N}^{k+1} \leftarrow \mathbf{Y} - \mathbf{X}^k$ 
17:      $\mathbf{N}^{k+1} \leftarrow \text{threshold}(|\mathbf{N}_{i,j}^{k+1}|_{i=1,j=1}^{m,n}, \beta_2 e^{-\alpha_2 k})$ 
18:      $\mathbf{X}^{k+1} \leftarrow \mathcal{D}(\mathbf{Y} - \mathbf{N}^{k+1})$ 
19:      $e \leftarrow \|\mathbf{N}^{k+1} - \mathbf{N}^k\|_F$ 
20:      $k \leftarrow k + 1$ 
21:   end while
22:   return  $\hat{\mathbf{X}} \leftarrow \mathbf{X}^k, \hat{\mathbf{N}} \leftarrow \mathbf{N}^k$ 
23: end procedure

```

first thresholded and then they are projected onto the set W ; however, in the modified version, the signal is first thresholded and an approximation of the sparse noise is derived according to (1), then this approximated noise is thresholded and a better estimation of the signal is found by (1). It should also be noted that two different threshold levels, **th1** and **th2**, are considered for signal and noise. **th1** and **th2** can be any decreasing sequences, but as is common in other papers [32], [33], we adopted the exponential scheme to decrease them in each iteration as shown below:

$$\begin{cases} \mathbf{th1}_k = \beta_1 e^{-\alpha_1 k} \\ \mathbf{th2}_k = \beta_2 e^{-\alpha_2 k} \end{cases} \quad (23)$$

The suitable setting for the four constants ($\alpha_1, \beta_1, \alpha_2$ and β_2) is discussed in the next section.

In the image processing context, the reconstruction is not perfect since images are not purely sparse by Discrete Cosine Transform (DCT) or other transforms used to make the images sparse such as Wavelet and Contourlet. Nevertheless, two pieces of side information are available, i.e., the signal values are in the interval $[0, 255]$ for 8-bit images and the signal contains a large low frequency component. We can take advantage of the first one and clip the estimated signal in each iteration. Since the thresholding function is non-linear and changes the range of the signal and noise, this modification will result in a better reconstruction. In other words, we are considering the matrices with entries in $[0, 255]$ and project our approximated signal onto this convex set in each iteration. Moreover, we can apply a low-pass filter, to the signal so as to emphasize the low-pass component of the image and attenuate the high frequency components of the noise. Various filters were tested such as gaussian filter, median/mean filter,

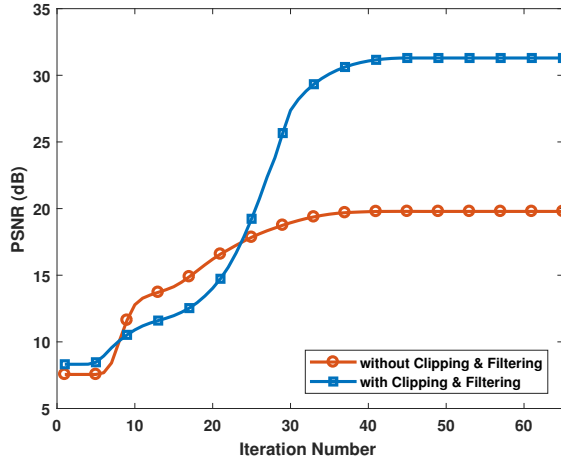


Fig. 1. Effect of clipping and filtering for the case of 50% salt-and-pepper noise for the Cropped Lena image.

cubic spline, non-local means [34] and guided image filter [35]. Gaussian filter was selected due to its best performance in our algorithm.

III. SIMULATION RESULTS

We evaluate the effectiveness of our algorithm for different scenarios, i.e., images, audio and artificial sparse signals. Simulations are conducted in MATLAB 2018a on a PC equipped with an Intel Core i-7 3.60GHZ CPU and 64-GB RAM.

A. Artificial Sparse Signal and Noise

In this subsection, we generate a 500×500 2-D signal which is sparse in DCT domain and a 500×500 sparse noise. The sparse elements of the signal and noise are independently sampled from a normal distribution with variance 128. We evaluate the performance of our algorithm in terms of Success Rate (SR) and SNR. A reconstruction is considered as a success if the output SNR is greater than 60 dB. The results are presented in Table I for different signal and noise sparsity ratios $\rho = \text{Sparsity Number}/500^2$. As can be seen in this table, when the sparsity ratio of both signal and noise are 30%, the success rate falls despite the fact that the average SNR is still high. As an example, let the sparsity ratio of one of the signals be 30%. Since the location and value of these entries are unknown, there are about 60% unknown variables and at least 60% equations are needed to find the unknown variables. If the location of the non-zero entries of the other signal was known, its sparsity ratio could have been 40%. However, in our case where no side information about the sparsity of the signals is provided, the sparsity ratio should be less than 40%.

Table I shows that when the signal and noise are purely sparse, our algorithm can fully reconstruct the signal.

B. Impulse Noise Removal from Images

The most common type of impulsive noise in image processing is salt-and-pepper noise. The noisy pixels in the image corrupted by this type of noise take the maximum or minimum

values of the image, i.e., zero or 255 in 8-bit-per-pixel images. Since images are almost sparse in the DCT domain, as an example of sparse noise removal from 2-D signals, we add salt-and-pepper noise to some images and employ Algorithm 2 for denoising. It is worth noting that we used other transformations making the images almost sparse such as Wavelet and Contourlet, and the Peak Signal to Noise Ratio (PSNR) was at most 0.2 dB better, but these transformations were more time-consuming. Therefore the results of the DCT transformation are reported. Furthermore, unknown missing samples are a special case of the salt-and-pepper noise (the probability of salt is zero) and the quality is about the same as that of salt-and-pepper noise.

The output PSNR for 256×256 cropped Lena image corrupted by 50% salt-and-pepper noise after each iteration of algorithm 2 with or without clipping plus gaussian filtering is depicted in Fig. 1. As can be seen, the clipping and gaussian filtering technique result in a better reconstruction both objectively and subjectively.

We compare our results with AMF [21] with maximum window size of 13, 7×7 DBA [22] and TPF [25]; The output PSNR values for the 512×512 images of *Lena*, *Baboon*, *Peppers*, and *Airplane* distorted with various densities of salt-and-pepper noise are depicted in Fig. 2.

Figures 3 and 4 exhibit the restored images of various methods for *Lena* and *Baboon* images corrupted by 60% salt-and-pepper noise, respectively.

As another example of sparse noise, we consider random-valued impulsive noise. In this case, each noisy pixel randomly takes a value in the interval $[0, 255]$ with uniform distribution. We compare our algorithm with the latest method [27] for random-valued impulsive noise removal from images. The results of our algorithm in comparison with the SAFE method can be found in Table II.

As can be seen in this table, our algorithm outperforms the SAFE method when the noise density is lower than 20% or higher than 60% and in other cases the difference between two methods is less than 1dB. The SAFE algorithm is not capable of reconstructing salt-and-pepper noise, and it is demonstrated in the next subsection that the run-time of our algorithm is much less than the SAFE method. The restored images for *Boat* image corrupted by respective 30% random-valued impulsive noise are depicted in Figure 5. It can be seen in these two figures that for low noise densities the output qualities are not much different but our algorithm preserve the details more, and for high noise densities the SAFE algorithm spread the noisy pixels as opposed to our algorithm, but preserve the edges better.

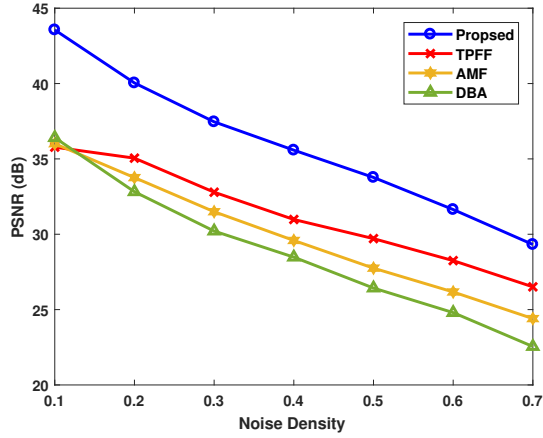
C. Complexity

We evaluate the complexity of our method in terms of the run-time in this subsection. The simulation is conducted for the *Lena* image corrupted with different densities of salt-and-pepper noise. The results are shown in Table III in comparison with MF, AMF, DBA, TPF, and SAFE.

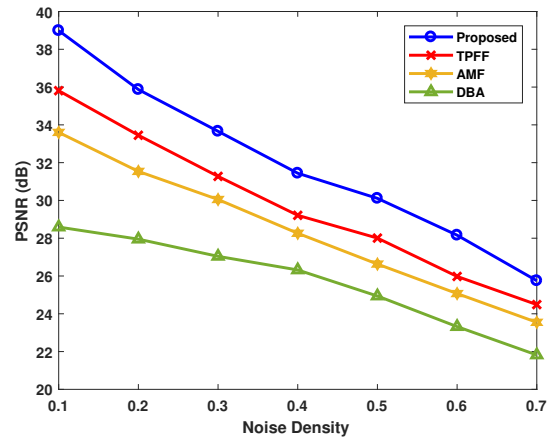
As can be seen in Table III, our method is very efficient and fast in restoring corrupted images with impulsive noise.

TABLE I
RECONSTRUCTION SNR (dB) AND SR (IN THE BRACKET) FOR DIFFERENT SIGNAL AND NOISE SPARSITY RATIOS (ρ)

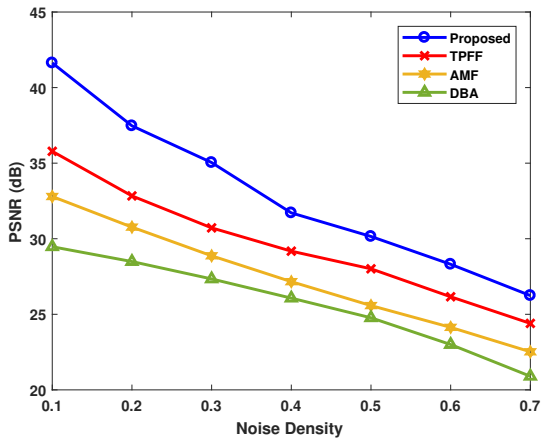
Noise Sparsity Ratio		10%	20%	30%
Signal Sparsity Ratio				
10%		316.5 (100%)	313.5 (100%)	311.6 (100%)
20%		315.9 (100%)	312.6 (100%)	310.4 (100%)
30%		314.9 (100%)	311.4 (100%)	224.082 (73%)



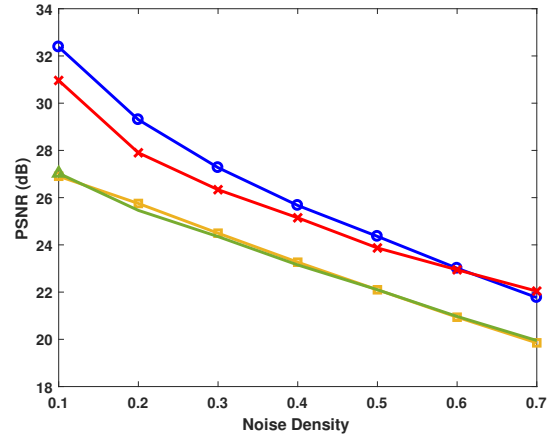
(a) Lena



(b) Peppers



(c) Airplane



(d) Baboon

Fig. 2. Comparison of restoration results in PSNR (dB) for various images corrupted by different densities of salt-and-pepper noise.

TABLE II
PSNR FOR DIFFERENT RANDOM-VALUED IMPULSIVE NOISE DENSITIES (ND)

		5% ND	10% ND	20% ND	30% ND	40% ND	50% ND	60% ND	70% ND	80% ND
Lena	SAFE	35.96	34.98	34.45	33.14	31.98	30.41	28.36	25.38	20.49
	Proposed	40.15	37.85	34.96	33.17	31.46	29.84	28.01	26.32	24.03
Boat	SAFE	32.23	31.21	30.17	29.11	28.03	26.46	25.11	22.83	19.09
	Proposed	35.1	32.99	30.65	29.12	27.65	26.07	25	23.42	21.54
Barbara	SAFE	29.69	29.27	27.9	26.97	25.86	24.35	22.96	21.09	17.79
	Proposed	34.07	30.81	27.66	25.46	24.39	23.53	22.83	22.08	20.6



Fig. 3. Reconstructed images using different methods for *Lena* image corrupted with 50% salt-and-pepper noise.(a)Original image, (b)Corrupted image, (c)AMF 13×13 , (d)DBA 7×7 , (e)TPDF, (f)Proposed.

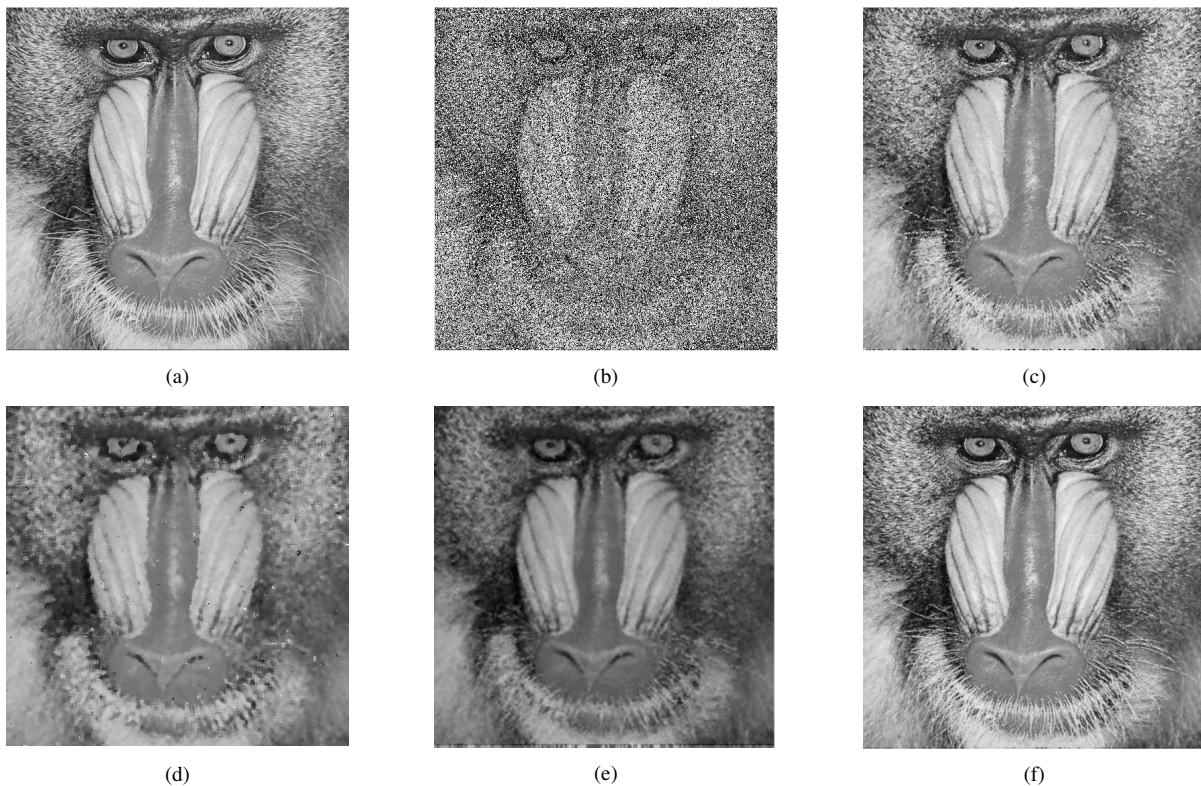


Fig. 4. Reconstructed images using different methods for *Baboon* image corrupted by 50% salt-and-pepper noise.(a)Original image, (b)Corrupted image, (c)AMF 13×13 , (d)DBA 7×7 , (e)TPDF, (f)Proposed.

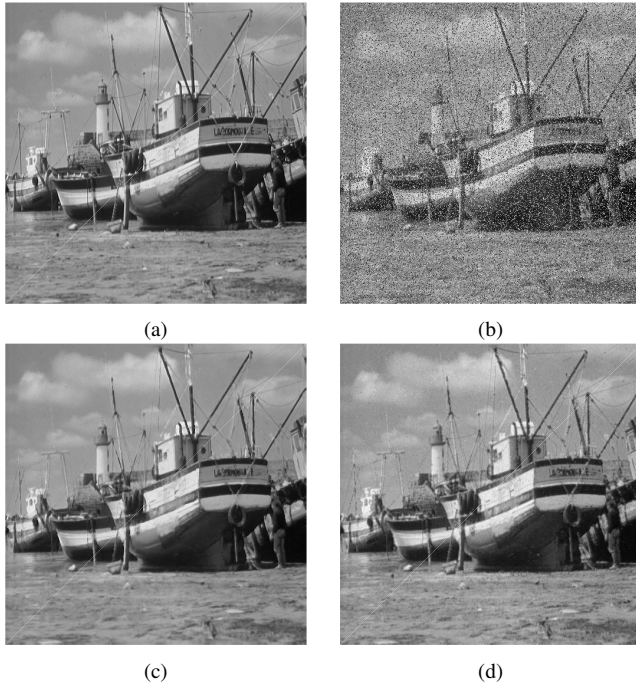


Fig. 5. Restored images for *Boat* image corrupted by 30% random-valued impulsive noise. (a) Original image, (b) Corrupted image, (c) SAFE, (d) Proposed.

TABLE III
RUN-TIME OF DIFFERENT METHODS IN SECONDS

Noise Density	Run-Time (sec)				
	Proposed	AMF	DBA	TPFF	SAFE(on GPU)
0.2	1.25	1.11	1.25	1.25	768.05(22.48)
0.3	1.25	1.13	1.25	1.75	763.48(23.85)
0.4	1.25	1.16	1.26	2.1	759.54(24.04)
0.5	1.25	1.24	1.27	2.5	753.5(31.95)
0.6	1.25	1.37	1.27	2.96	749.61(39.74)

The complexity of our algorithm is only dependent on the dimension of the signals since the noise level does not impact the number of iterations of our method. In each iteration of the proposed method, there are one 2D-DCT, one 2D-IDCT, two thresholding, one clipping and one gaussian filtering. The complexities of 2D-DCT and 2D-IDCT are $\mathcal{O}(n^2 \log n)$, where the signals are assumed to be $n \times n$ (running 1D-DCT $2n$ times each with complexity $\mathcal{O}(n \log n)$ [36]). The computation complexity of thresholding is $\mathcal{O}(n^2)$, Finally, for gaussian filter one can apply FFT and IFFT with complexity $\mathcal{O}(n \log n)$; hence the overall complexity of our algorithm is $\mathcal{O}(n^2) \log n$ regardless of the noise density.

IV. CONCLUSION

In this paper, we proposed a new method for sparse noise removal from sparse signals. The sparsity domains of the signal and noise were assumed to be different. An optimization problem was suggested and was solved by iteratively thresholding the estimated signal and noise in their sparsity domains. Furthermore, some modifications to the original method were presented to improve the reconstruction quality. We

evaluated different aspects of our method through numerical experiments with comparison to other well-known methods. We observed that our algorithm is fast and suitable for real-time applications and it outperforms other methods in terms of reconstruction quality and/or complexity. Additionally, the proposed algorithm works for i-D and 2-D signals that are corrupted by salt-and-pepper noise, random-valued impulsive noise and unknown random missing samples as opposed to other well-known methods that are for either salt-and pepper or random valued impulsive noise.

For Future work, we can consider removal of sparse noise from videos, image inpainting and block sparse noises such as block losses in the JPEG and MPEG images. For such cases, we have to employ block-sparse recovery methods.

REFERENCES

- [1] S. Zahedpour, S. Feizi, A. Amini, M. Ferdosizadeh, and F. Marvasti, "Impulsive noise cancellation based on soft decision and recursion," *IEEE Transactions on instrumentation and measurement*, vol. 58, no. 8, pp. 2780–2790, 2009.
- [2] H. Hosseini, F. Hesar, and F. Marvasti, "Real-time impulse noise suppression from images using an efficient weighted-average filtering," *IEEE Signal Processing Letters*, vol. 22, no. 8, pp. 1050–1054, 2015.
- [3] R. Rajagopalan and B. Subramanian, "Removal of impulse noise from audio and speech signals," in *Signals, Circuits and Systems, 2003. SCS 2003. International Symposium on*, vol. 1. IEEE, 2003, pp. 161–163.
- [4] M. G. Sanchez, L. De Haro, M. C. Ramón, A. Mansilla, C. M. Ortega, and D. Oliver, "Impulsive noise measurements and characterization in a uhf digital tv channel," *IEEE Transactions on electromagnetic compatibility*, vol. 41, no. 2, pp. 124–136, 1999.
- [5] R. H. Chan, C.-W. Ho, and M. Nikolova, "Salt-and-pepper noise removal by median-type noise detectors and detail-preserving regularization," *IEEE Transactions on image processing*, vol. 14, no. 10, pp. 1479–1485, 2005.
- [6] K. K. V. Toh and N. A. M. Isa, "Noise adaptive fuzzy switching median filter for salt-and-pepper noise reduction," *IEEE signal processing letters*, vol. 17, no. 3, pp. 281–284, 2010.
- [7] C. Spinola, A. Gago, J. Bonelo, and J. Vizoso, "Filtering of impulse noise from laser sensor signals in the process of non-contact thickness measurement in a stainless steel sheet production line," in *Instrumentation and Measurement Technology Conference, 2000. IMTC 2000. Proceedings of the 17th IEEE*, vol. 3. IEEE, 2000, pp. 1303–1307.
- [8] N. Kim, H.-G. Byun, Y.-H. You, and K. Kwon, "Blind signal processing for impulsive noise channels," *Journal of Communications and Networks*, vol. 14, no. 1, pp. 27–33, 2012.
- [9] M. Zimmermann and K. Dostert, "Analysis and modeling of impulsive noise in broad-band powerline communications," *IEEE transactions on Electromagnetic compatibility*, vol. 44, no. 1, pp. 249–258, 2002.
- [10] F. Marvasti, *Nonuniform sampling: theory and practice*. Springer Science & Business Media, 2012.
- [11] N. Zarmehi and F. Marvasti, "Sparse and low-rank recovery using adaptive thresholding," *Digital Signal Processing*, vol. 73, pp. 145–152, 2018.
- [12] —, "Adaptive singular value thresholding," in *Sampling Theory and Applications (SampTA), 2017 International Conference on*. IEEE, 2017, pp. 442–445.
- [13] S. Oymak, A. Jalali, M. Fazel, Y. C. Eldar, and B. Hassibi, "Simultaneously structured models with application to sparse and low-rank matrices," *IEEE Transactions on Information Theory*, vol. 61, no. 5, pp. 2886–2908, 2015.
- [14] S. Esakkirajan, T. Veerakumar, A. N. Subramanyam, and C. Premchand, "Removal of high density salt and pepper noise through modified decision based unsymmetric trimmed median filter," *IEEE Signal processing letters*, vol. 18, no. 5, pp. 287–290, 2011.
- [15] A. Adler, V. Emiya, M. G. Jafari, M. Elad, R. Gribonval, and M. D. Plumbley, "Audio inpainting," *IEEE Transactions on Audio, Speech, and Language Processing*, vol. 20, no. 3, pp. 922–932, 2012.
- [16] A. Roy, J. Singha, S. S. Devi, and R. H. Laskar, "Impulse noise removal using svm classification based fuzzy filter from gray scale images," *Signal Processing*, vol. 128, pp. 262–273, 2016.

- [17] V. Gupta, V. Chaurasia, and M. Shandilya, "Random-valued impulse noise removal using adaptive dual threshold median filter," *Journal of Visual Communication and Image Representation*, vol. 26, pp. 296–304, 2015.
- [18] X. Zhang and Y. Xiong, "Impulse noise removal using directional difference based noise detector and adaptive weighted mean filter," *IEEE Signal processing letters*, vol. 16, no. 4, pp. 295–298, 2009.
- [19] J. Wu and C. Tang, "Pde-based random-valued impulse noise removal based on new class of controlling functions," *IEEE transactions on image processing*, vol. 20, no. 9, pp. 2428–2438, 2011.
- [20] F. Ahmed and S. Das, "Removal of high-density salt-and-pepper noise in images with an iterative adaptive fuzzy filter using alpha-trimmed mean," *IEEE Trans. Fuzzy Systems*, vol. 22, no. 5, pp. 1352–1358, 2014.
- [21] H. Hwang and R. A. Haddad, "Adaptive median filters: new algorithms and results," *IEEE Transactions on image processing*, vol. 4, no. 4, pp. 499–502, 1995.
- [22] K. Srinivasan and D. Ebenezer, "A new fast and efficient decision-based algorithm for removal of high-density impulse noises," *IEEE signal processing letters*, vol. 14, no. 3, pp. 189–192, 2007.
- [23] A. Ba, M. E. YÜksel *et al.*, "Impulse noise removal from digital images by a detail-preserving filter based on type-2 fuzzy logic," *IEEE Transactions on Fuzzy Systems*, vol. 16, no. 4, pp. 920–928, 2008.
- [24] F. R. Avila and L. W. Biscainho, "Bayesian restoration of audio signals degraded by impulsive noise modeled as individual pulses," *IEEE Transactions On Audio, Speech, And Language Processing*, vol. 20, no. 9, pp. 2470–2481, 2012.
- [25] H.-H. Chou, L.-Y. Hsu, and H.-T. Hu, "Turbulent-pso-based fuzzy image filter with no-reference measures for high-density impulse noise," *IEEE transactions on cybernetics*, vol. 43, no. 1, pp. 296–307, 2013.
- [26] J. Wu and C. Tang, "Random-valued impulse noise removal using fuzzy weighted non-local means," *Signal, Image and Video Processing*, vol. 8, no. 2, pp. 349–355, 2014.
- [27] Y. Chen, Y. Zhang, J. Yang, H. Shu, L. Luo, J.-L. Coatrieux, and Q. Feng, "Structure-adaptive fuzzy estimation for random-valued impulse noise suppression," *IEEE Transactions on Circuits and Systems for Video Technology*, 2016.
- [28] T. Chen and H. R. Wu, "Adaptive impulse detection using center-weighted median filters," *IEEE Signal Processing Letters*, vol. 8, no. 1, pp. 1–3, 2001.
- [29] J. Jiang, L. Zhang, and J. Yang, "Mixed noise removal by weighted encoding with sparse nonlocal regularization," *IEEE transactions on image processing*, vol. 23, no. 6, pp. 2651–2662, 2014.
- [30] K. H. Jin and J. C. Ye, "Sparse and low-rank decomposition of a hankel structured matrix for impulse noise removal," *IEEE Transactions on Image Processing*, vol. 27, no. 3, pp. 1448–1461, 2018.
- [31] D. L. Donoho and X. Huo, "Uncertainty principles and ideal atomic decomposition," *IEEE transactions on information theory*, vol. 47, no. 7, pp. 2845–2862, 2001.
- [32] M. Azghani, P. Kosmas, and F. Marvasti, "Microwave medical imaging based on sparsity and an iterative method with adaptive thresholding," *IEEE transactions on medical imaging*, vol. 34, no. 2, pp. 357–365, 2015.
- [33] H. Zamani, H. Zayyani, and F. Marvasti, "An iterative dictionary learning-based algorithm for doa estimation," *IEEE Communications Letters*, vol. 20, no. 9, pp. 1784–1787, 2016.
- [34] A. Buades, B. Coll, and J.-M. Morel, "A non-local algorithm for image denoising," in *Computer Vision and Pattern Recognition, 2005. CVPR 2005. IEEE Computer Society Conference on*, vol. 2. IEEE, 2005, pp. 60–65.
- [35] K. He, J. Sun, and X. Tang, "Guided image filtering," *IEEE transactions on pattern analysis & machine intelligence*, no. 6, pp. 1397–1409, 2013.
- [36] N. Ahmed, T. Natarajan, and K. R. Rao, "Discrete cosine transform," *IEEE transactions on Computers*, vol. 100, no. 1, pp. 90–93, 1974.